ECS Transactions, 86 (1) 55-63 (2018)
10.1149/08601.0055ecst ©The Electrochemical Society

Light Enhanced Metal Assisted Chemical Etching of Silicon

E. Quiroga-González[a*], M. A. Juárez-Estrada[b], and E. Gómez-Barojas[b]

[a] Institute of Physics, Benemérita Universidad Autónoma de Puebla, Puebla 72570, Mexico
[b] Semiconductor Device Research Center, Benemérita Universidad Autónoma de Puebla, Puebla 72570, Mexico

The effects of backside illumination during Metal Assisted Chemical Etching of Silicon are here discussed. Photoluminescence, Raman spectroscopy and SEM have been used to elucidate the morphological changes when illumination is applied. n and p type Silicon wafers have been used to prove the concept, obtaining similar results: Faster etching rates and lateral porosification.

Introduction

The interest in porous Si (PSi), and particularly in its nanostructure, exploded in the early 1990s when Leigh Canham reported efficient, bright red-orange photoluminescence from the material, and almost simultaneously Ulrich Gössele identified quantum confinement effects in the absorption spectrum of PSi (1, 2). This quantum confinement is mainly due to the rough walls of the pores in silicon (structures of nano-size).

As PSi can be prepared in the form of micro-, meso- and macro-pores, it has been used as active material for chemical sensors (3). Additionally, it has been proposed as a promising material as a drug delivery vehicle for medicaments such as steroid dexamethasone (4) and ibuprofen (5). Likewise, PSi is very promising in the field of energy storage as anode in high-performance lithium batteries (6).

PSi is mainly fabricated by electrochemical etching in presence of hydrofluoric acid, water and an oxidizing agent like ethanol. The modulation of porosity is obtained by varying process parameters like current density and illumination, where this last parameter is important in the generation of electron-hole pairs necessary for the etching process in n-type Si (7-9). Alternatively to electrochemical etching, in the last years, some another synthesis routes to obtain PSi have been employed; one of those is Metal Assisted Chemical Etching (MACE) (10-12). This method does not need a voltage source for etching, because the particles deposited onto the silicon wafer form a Schottky barrier, which acts as an internal voltage source. With this technique different forms and porosities can be obtained, just as in the case of electrochemical etching (9). Nevertheless, there is no evidence of MACE using backside illumination during the etching process, even when it is known that illumination is needed for etching macropores electrochemically in n-type Si. Using light could bring more flexibility to the MACE process. The aim of this work is to porosify n and p type silicon employing the MACE process, applying light during the synthesis.

Experimental details

For the experiments, p-type Si wafers with resistivity of 15-25 Ωcm, and n-type Si wafers with resistivity of 0.03-0.05 Ωcm were used. Their thickness is 550 μm. With these wafers, electronic hole concentrations of 10^{15} and 10^{3} cm^{-3} are available, respectively. These medium and low concentrations are planned for better observing the effect of photogenerated holes.

In the present work, MACE was performed using Ag particles as catalyst. The particles were chemically deposited on the Si wafers. Two different concentrations of $AgNO_3$ in aqueous solution were used for the deposition of Ag particles: 0.002 y 0.006 M. The final plating solution contained 26.3 mL of the solution of $AgNO_3$, 0.5 mL of HF 48%, 0.8 mL of H_2O_2 and 0.125 g polyethylenglycol 3600. HF reacts with Si or SiO_2 (Si oxidized with H_2O_2) producing H_2SiF_6 and liberating electrons. These electrons reduce the Ag^+ ions from $AgNO_3$ producing Ag^0 on the surface of Si. Pieces of wafer of around 1 cm^2 were immersed in the plating solution under agitation in an ultrasonic bath for 6 s at 25 °C. After deposition, the Si pieces were rinsed with deionized water and dried with N_2 flux.

To produce PSi, the pieces of Si were fixed at the bottom of a Teflon container with a perforation. Through the perforation illumination was applied at a distance of 0.5 mm. The light source was a red LED of 10 W, with an emission band centered at 800 nm, covering a portion of the near infrared range. The etching solution was composed of 2 mL of HF 48%, 3 mL of H_2O_2 and 20 mL of H_2O. H_2O_2 decomposes in the presence of Ag particles, liberating electronic holes, which are needed for the etching process (to produce SiO_2, which is dissolved by HF). All the samples were submitted to etching without illumination for 30 s, followed by 30 min etching with or without illumination. The temperature of the etchant was kept around 30 °C throughout the etching process with a cooling fan. After etching, the Si pieces were rinsed with deionized water and dried with N_2 flux.

The morphology of the samples was analyzed by SEM microscopy. For this purpose, a field emission SEM JSM-7800F of JEOL was used. Photoluminescence spectra were recorded at room temperature with a spectrofluorometer Horiba Nano Log, using a 35° optical geometry. The samples were excited at 300 nm, using an additional band pass filter of 400 nm. Raman spectra of the samples were recorded using a Raman microscope Horiba LabRam HR, with a 632 nm laser, using a 100x objective.

Results and discussion

Morphology

Figure 1 a) and b) shows micrographs of Ag particles deposited using a solution 0.002 M of $AgNO_3$, on n and p type Si, respectively. As can be observed, the distribution of sizes and shapes is very similar for both doping types. The diameter of the particles ranges from 6 to 27 nm (the average diameter is 16 nm). In the same form, the Ag particles deposited using a solution 0.006 M of $AgNO_3$ are very similar in shapes and sizes independently of the doping type (see Figure 1 c) for n-type, and d) for p-type). The diameter of these particles ranges from 22 to 55 nm (the average diameter is 38 nm).

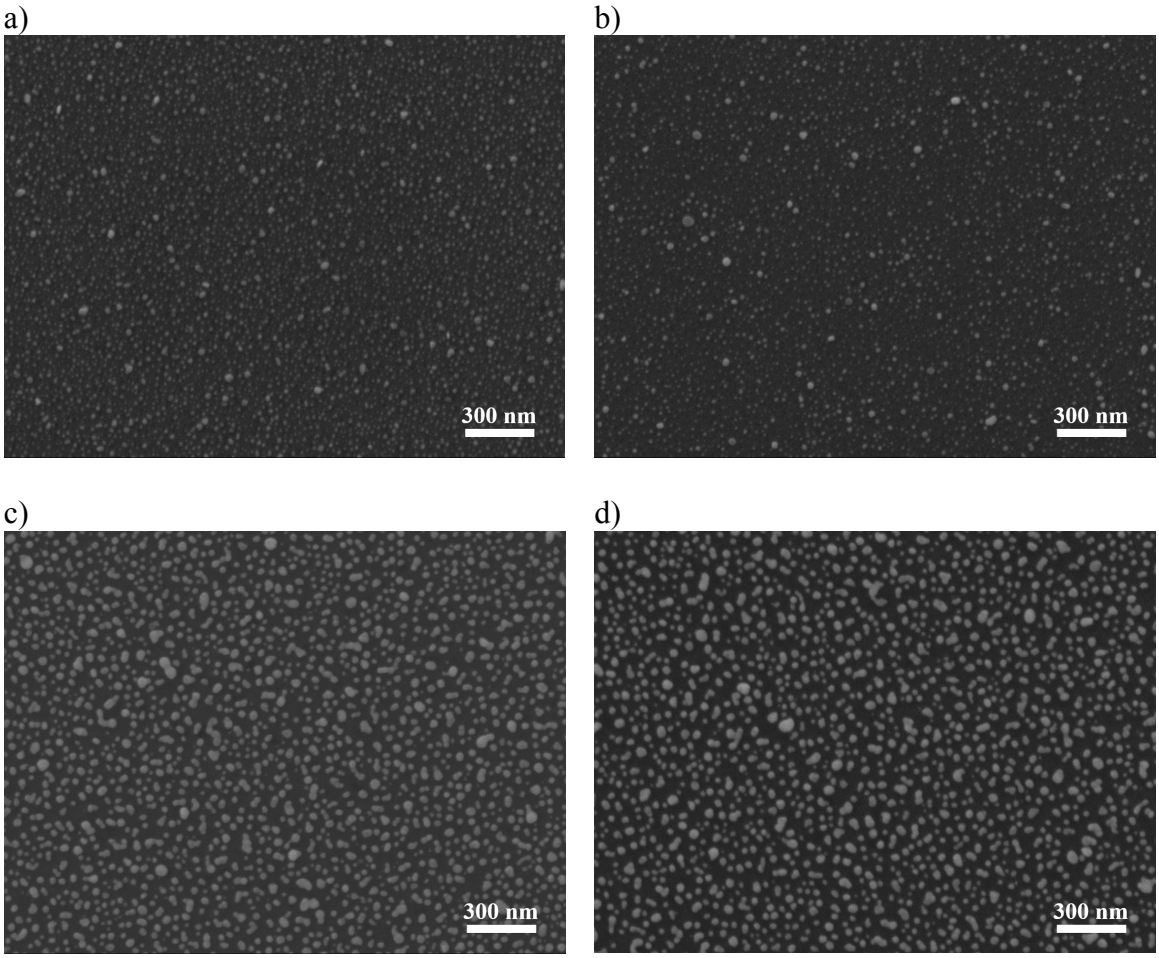

Figure 1. SEM micrographs of Ag particles chemically deposited on Si; using a 0.002 M solution of $AgNO_3$: a) On n-type Si, and b) on p-type Si; using a 0.006 M solution of $AgNO_3$: c) On n-type Si, and d) on p-type Si.

As evidenced before from the micrographs of Figure 1, two average sizes of Ag particles are identified: 16 and 38 nm. Pores were etched in n and p type Si by MACE with those particles.

Figure 2 shows SEM micrographs of pores obtained in n-type Si. a) and b) show pores etched with Ag particles of 16 nm, under darkness and illumination, respectively. c) and d) show pores etched with Ag particles of 38 nm, under darkness and illumination, respectively.

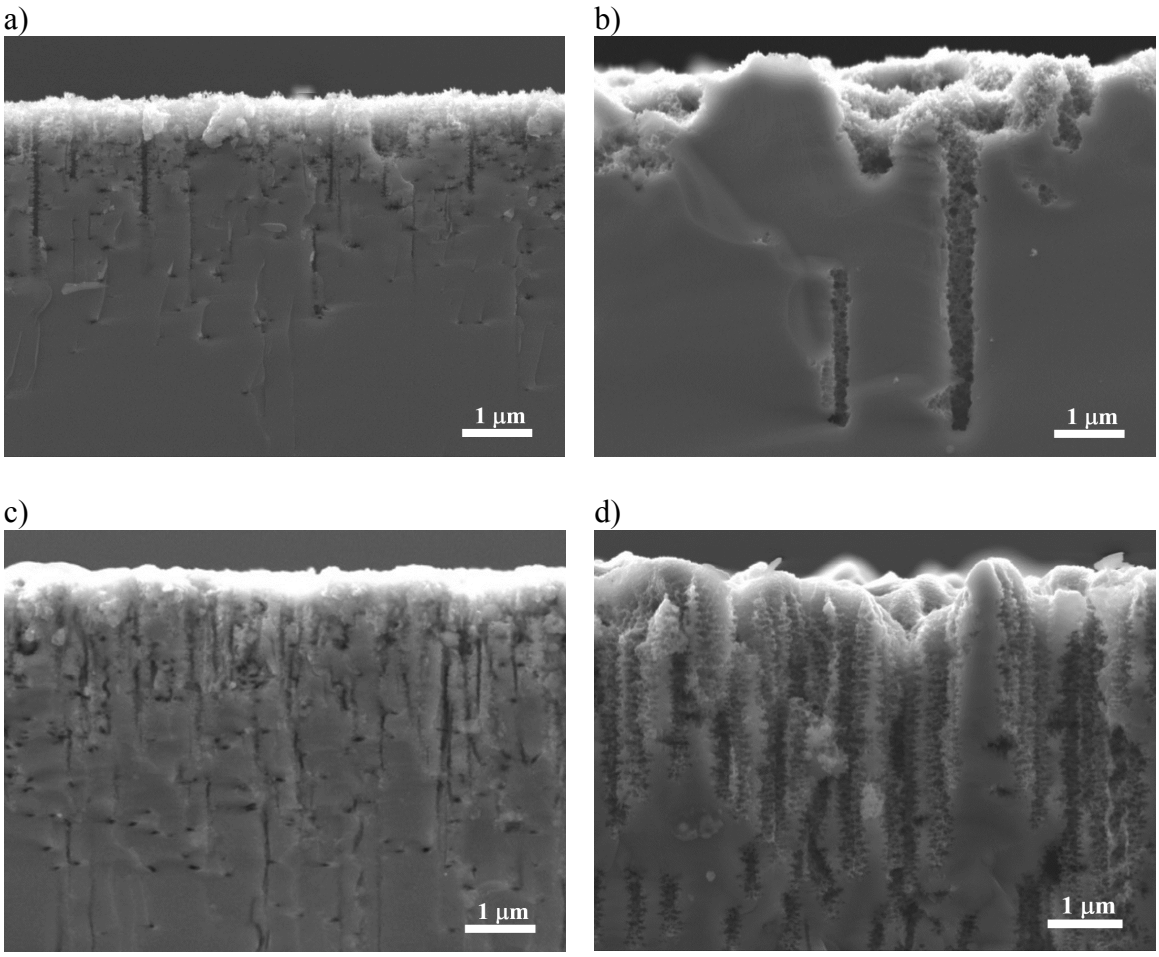

Figure 2. SEM micrographs of porosified n-type Si. Etched with Ag particles of 16 nm: a) under darkness, and b) under illumination. Etched with Ag particles of 38 nm: c) under darkness, and d) under illumination.

Figure 3 shows SEM micrographs of pores obtained in p-type Si. a) and b) show pores etched with Ag particles of 16 nm, under darkness and illumination, respectively. c) and d) show pores etched with Ag particles of 38 nm, under darkness and illumination, respectively.

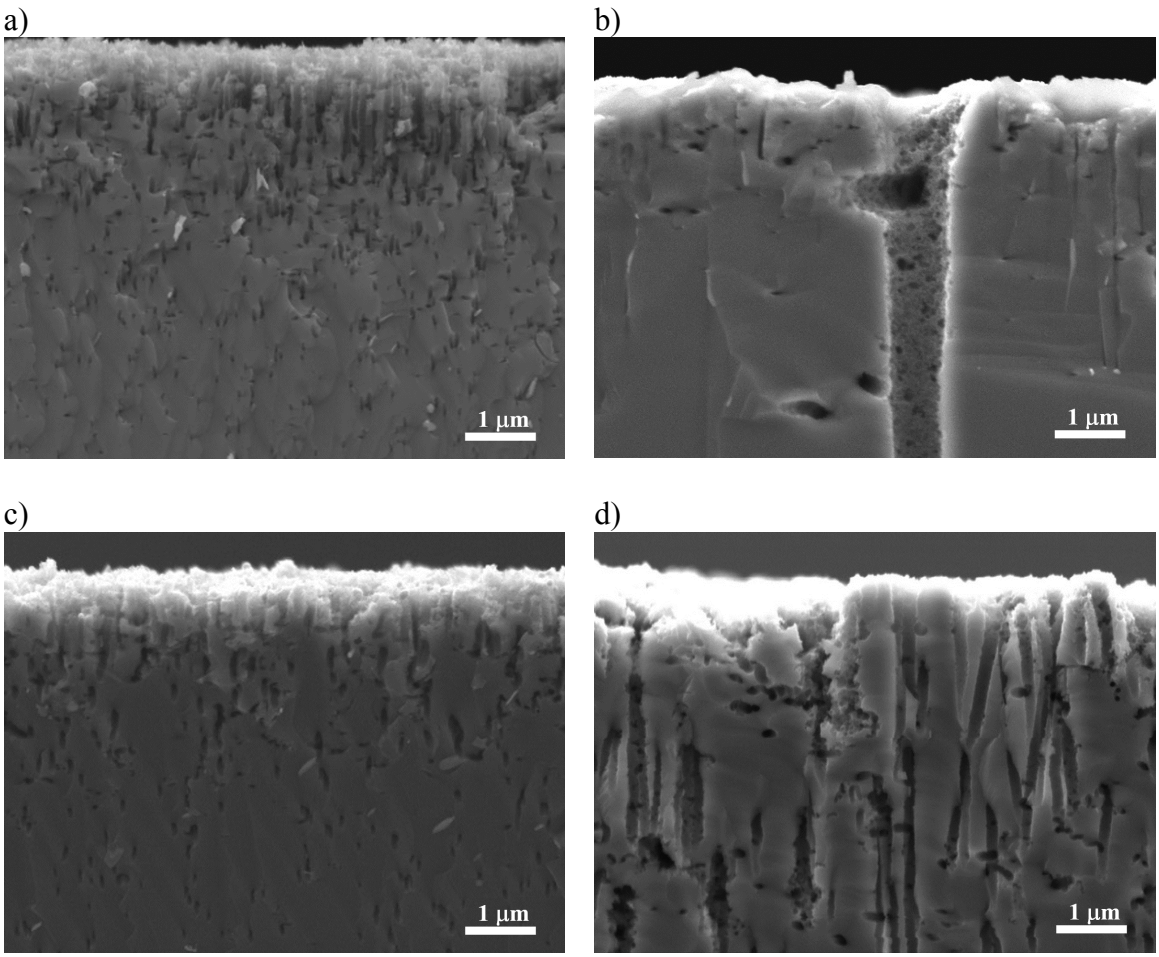

Figure 3. SEM micrographs of porosified p-type Si. Etched with Ag particles of 16 nm: a) under darkness, and b) under illumination. Etched with Ag particles of 38 nm: c) under darkness, and d) under illumination.

From micrographs captured at lower magnifications it was possible to determine the depth of the pore front. Table I summarizes the pore front depths for all the PSi samples.

TABLE I. Pore front depths of all produced PSi samples.

Substrate	Illumination	Pore front depth [μm]
n-type (Ag = 16 nm)		9.0
n-type (Ag = 16 nm)	X	14.4
n-type (Ag = 38 nm)		10.9
n-type (Ag = 38 nm)	X	17.1
p-type (Ag = 16 nm)		8.5
p-type (Ag = 16 nm)	X	20.6
p-type (Ag = 38 nm)		7.7
p-type (Ag = 38 nm)	X	27.5

It is evident that the etching rate for n-type Si increases about 1.6 times when illumination is applied, while it increases in average 3 times for p-type Si. This can be attributed to the photogenerated electronic holes (h+). In the case of n-type Si the vertical etching rate does not increase as much as in p-type Si, because lateral etching is

prominent in this case. As can be observed in Figure 2 d), macrocavities are evident in the pore walls of PSi etched in n-type Si with 38 nm Ag particles.

Figure 4 a) shows a schematic of the energy bands of the n-type Si - Ag junction. As can be observed, a space charge region (SCR) is formed at the metal-semiconductor interface, due to the difference between the work function of Ag (4.26 eV) and the electron affinity of Si (4.01 eV) (13). There is a barrier for holes coming from the electrolyte, thus etching proceeds around the metal particles and not below them, as schematized in Figure 4 b); a pore with an Ag particle and etchant solution is shown in this figure. A contrasting scenario occurs with p-type Si, where a barrier is formed, but for holes coming from the semiconductor (see Figure 4 c)); however, this SCR acts as an accelerating potential for holes from the electrolyte into the semiconductor, allowing vertical etching (see Figure 4 d). Lateral etching is enabled when illumination is applied, especially with larger Ag particles. As in the case of n-type Si, with smaller particles (16 nm particles, in this work), the small contact area produces omnidirectional etching. This proceeds until coalescence of particles is reached (big Ag agglomerates are formed randomly) allowing vertical etching.

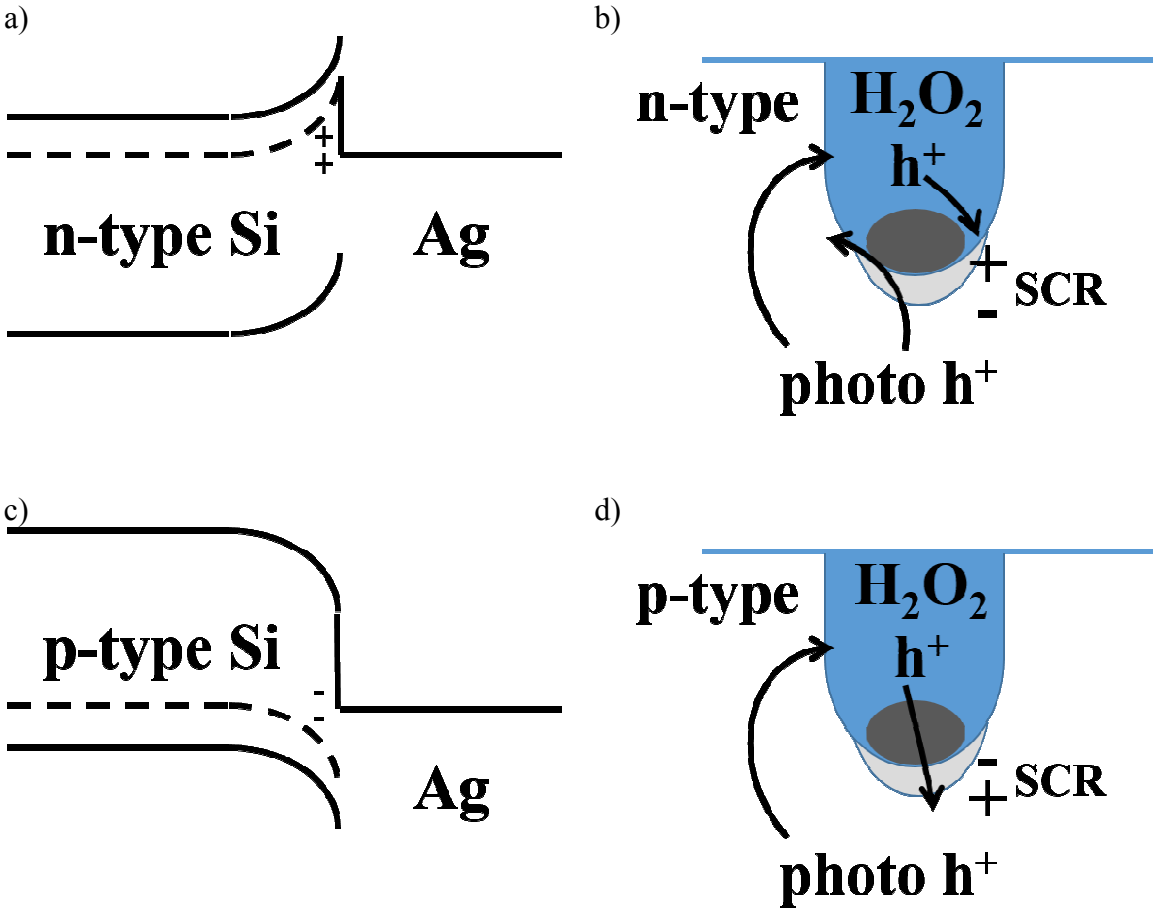

Figure 4. a) Band diagram of the n-type Si – Ag junction. b) Schematic of the MACE process with n-type Si and Ag. c) Band diagram of the p-type Si – Ag junction. d) Schematic of the MACE process with p-type Si and Ag.

Raman microscopy

The most prominent Raman peak of Si, located at about 521 cm^{-1} (TO mode at the center of the Brillouin zone) was tracked to analyze its asymmetry. It has been reported that the presence of nanocrystalline Si, or nanometric Si features may induce an asymmetry of this peak, and this asymmetry can be used to estimate nanocrystallite sizes (14). A measure of asymmetry is the ratio LWHM/RWHM (Left Width at Half Maximum / Right Width at Half Maximum); however, as the asymmetry is not pronounced in the present samples, the widths were taken at a quarter of the maximum (the ratio is then LWQM / RWQM) to have larger values and reduce errors. Figure 5 shows a typical Raman spectrum of the PSi samples. The measured parameters are indicated in the figure.

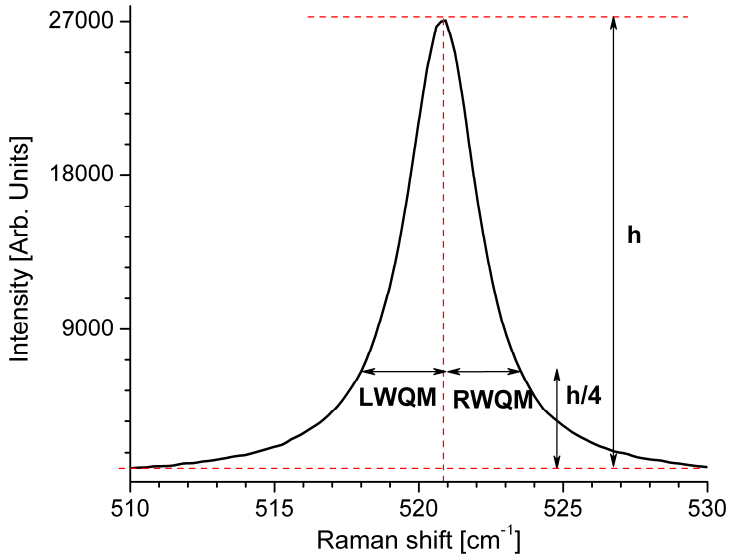

Figure 5. Typical Raman spectrum of PSi of this work. The tracked parameters are indicated in the figure.

Figure 6 shows plots of the ratio LWQM/RWQM for the PSi samples with a) n-type substrate, and b) p-type substrate. As can be observed, the asymmetry reduces with illumination in n-type samples, and it is contrary for p-type samples. This is in accordance with the SEM analysis, where it was evidenced that lateral porosification intensifies in n-type Si when illumination is applied, producing macro-cavities instead of mesoporosity with thinner pore walls. In the case of p-type Si, lateral mesoporification occurs when illumination is applied, thus the asymmetry of the Raman peak increases. There is the same tendency for the two different sizes of Ag particles used for the etching process, even when the density of macropores reduces drastically when smaller particles are used. This happens because there is a homogeneous porosity at the surface of the samples, where the beam of the Raman microscope was focused.

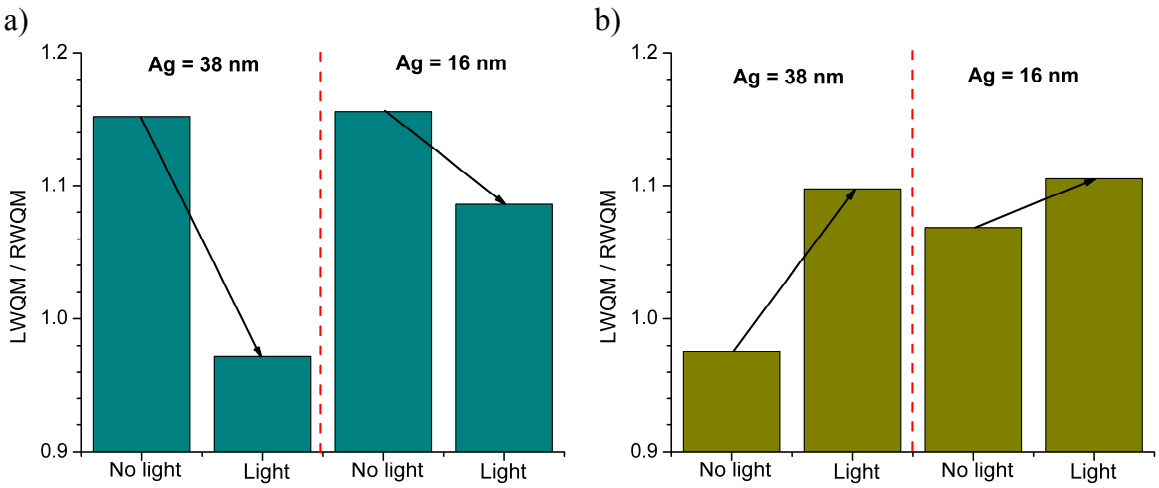

Figure 6. Plots of the ratio LWQM/RWQM for the PSi samples with a) n-type substrate, and b) p-type substrate.

Photoluminescence

Figure 7 shows a comparative of the photoluminescence (PL) spectra of PSi etched in a) n-type Si, and b) p-type Si. The PL spectra of all the PSi samples present the same 3 broad bands at about 620, 665 and 810 nm. This indicates that PL of all the samples has the same origin. As the position of the bands is independent of the morphology and size of the pores, the origin must be different kinds of surface defects. The intensity of the bands increases with illumination. The bigger contrast in intensity is obtained comparing the samples prepared with Ag particles of 16 nm, with and without illumination. This happens because the first couple of microns (in the range of the penetration length of the excitation radiation of 300 nm) of the samples produced with illumination have a high density of randomly-oriented mesopores (providing a large net surface area), in contrast to the individual vertical mesopores obtained without illumination.

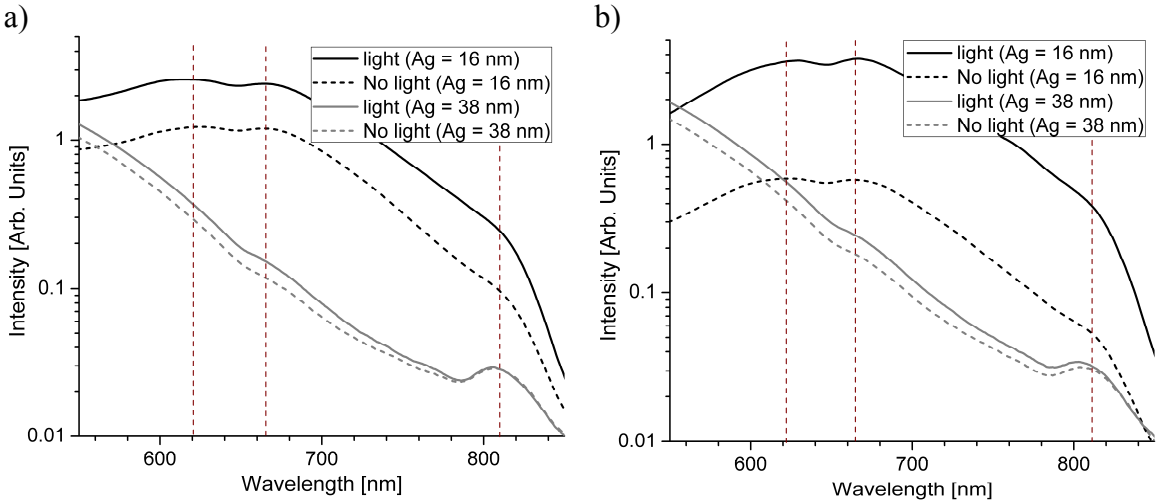

Figure 7. Photoluminescence spectra of PSi samples with a) n-type substrate, and b) p-type substrate.

Conclusion

Si porosification via Metal Assisted Chemical Etching has been modified for the first time using backside illumination, for both n- and p-type Si substrates. The etching rate increases about 1.6 times in n-type Si, and about 3 times in p-type Si. The lower rates in n-type Si are caused by lateral etching. The density and shape of the pores also depends on the size of the Ag catalyst particles, favoring vertical or lateral etching.

The intensity of the photoluminescence of PSi obtained under illumination could be enhanced even an order of magnitude, compared with its counterpart prepared without illumination. The use of backside illumination gives an extra freedom degree to the Metal Assisted Chemical Etching process.

Acknowledgments

This work was funded by projects CONACyT CB-2014-01-243407 and 100523072-VIEP2018. M. A. Juárez-Estrada acknowledges the financial support of CONACyT through a scholarship.

References

1. L. T. Canham, *Appl. Phys. Lett.*, **57**(10), 1046 (1990).
2. V. Lehmann and U. Gösele, *Appl. Phys. Lett.*, **58**(8), 856 (1991).
3. R. C. Anderson, R. S. Müller and C. W. Tobias, *Sens. Actuators A*, **23**, 835 (1990).
4. E. J. Anglin, M. P. Schwartz et al., *Langmuir*, **20**, 1126 (2004).
5. C. Charnay, S. Begu et al., *Eur. J. Pharm.* **57**, 533 (2004).
6. H. Kim et al., *Angew. Chem.*, **120**(54), 10305 (2008).
7. H. Ohji, P. J. Trimp and P. J. French, *Sens. Actuators A*, **73**(1), 95 (1999).
8. E. Quiroga-González and H. Föll, in Porous Silicon from Formation to Application. Vol. One, G. Korotcenkov, Editor, p. 25, CRC Press, London (2015).
9. A. L. Cheng, C. H. Chung and H. C. Lee, *J. Electrochem. Soc.*, **155**(11), D711 (2008).
10. É. Vázsonyi, E. Szilágyi, P. Petrik, Z. Horváth, T. Lohner, M. Fried and G. Jalsovsky, *Thin Solid Films*, **388**, 295 (2001).
11. R. Hummel and S. Chang, *Appl. Phys. Lett.*, **61**(16), 1965 (1992).
12. Z. Huang et al., *Adv. Mater.*, **23**(2), 285 (2011).
13. CRC Handbook of Chemistry and Physics, p. 12-114, CRC Press, London (2008).
14. E. Quiroga, W. Bensch, M. Aceves, Z. Yu, J. P. Savy, M. Haeckel and A. Lechner, in IEEE proceedings of the 10th international conference on ultimate integration of silicon, p. 349, Aachen, Germany (2009).